

## Hydrogen Peroxide Biosensor Based on Graphene-Toluidine Blue/HRP-Poly (Toluidine Blue)

Shaoming Yang\*, Shaoqing Ding, Lingling Li, Qing Sun, Jie Yang, Qiang Cao

School of Materials Science and Engineering, East China Jiaotong University, Nanchang 330013, Jiangxi, China

\*E-mail address: [yangsm79@163.com](mailto:yangsm79@163.com), [yangsm@aliyun.com](mailto:yangsm@aliyun.com)

*Received:* 1 August 2017 / *Accepted:* 12 September 2017 / *Published:* 12 October 2017

A novel hydrogen peroxide biosensor was prepared by entrapping horseradish peroxidase (HRP) by electropolymerization of toluidine blue onto a graphene-toluidine blue nanocomposite-modified base electrode. Graphene and the graphene-toluidine blue nanocomposites were characterized by SEM and UV-Vis spectroscopy. The preparation of the biosensor was monitored using electrochemical impedance spectroscopy. The catalytic performances of the biosensor were investigated using cyclic voltammetry and chronoamperometry. The performance of the biosensor was evaluated, and the results indicated that the biosensor exhibited excellent catalytic performance for the detection of hydrogen peroxide. The linear response range of the biosensor for hydrogen peroxide was  $5.0 \times 10^{-7} \sim 1.35 \times 10^{-5}$  mol·L<sup>-1</sup> with a sensitivity of 4.32 μA·L·μmol<sup>-1</sup>, a correlation coefficient of 0.999 and a detection limit of  $3.5 \times 10^{-7}$  mol·L<sup>-1</sup> (S/N=3).

**Keywords:** enzyme electrode, hydrogen peroxide, horseradish peroxidase, toluidine blue, biosensor

### 1. INTRODUCTION

Graphene (Gr) is a two-dimensional carbon-based material with a large surface area, high conductivity, good stability, mechanical strength and biocompatibility. Graphene has been widely applied in the field of electrochemical biosensors [1, 2]. However, due to the strong  $\pi \rightarrow \pi$  interactions between the graphene sheets, graphene is prone to aggregation and precipitation in solutions, thereby limiting its applications for electrochemical biosensors. Therefore, it is necessary to conduct covalent or non-covalent functionalization of graphene to permit the dispersion of graphene in solution [3]. Covalent functionalization can destroy the original structure of graphene and affect its intrinsic properties. However, because non-covalent functionalization can preserve the intrinsic properties of

graphene, this process has attracted considerable attention [4-6]. For example, thionine was selected to non-covalently functionalize graphene to promote the dispersion of graphene in solution because of the strong  $\pi\rightarrow\pi$  interactions between graphene and the planar aromatic ring structure of thionine [6].

Thionine, toluidine blue (TB) and methylene blue, which are redox electron mediators, can be exploited for the non-covalent functionalization of graphene. On one hand, these mediators can promote the dispersion of graphene in solution. On the other hand, due to the large specific surface area, high conductivity and good biocompatibility of graphene combined with the excellent electrocatalytic and rapid electron transfer properties of the electron mediators, high sensitivity electrochemical sensors can be developed [6-10]. For example, Wang et al. [7] and Zhang et al. [8], prepared electrodes that were modified with methylene blue-functionalized graphene that exhibited good catalytic performances for hydrogen peroxide and NADH.

Enzyme sensors are the most representative sensors among electrochemical biosensors with good selectivity, a rapid response and high sensitivity. The enzyme immobilization process is a key aspect of the preparation of enzyme sensors. A variety of techniques have been used for enzyme immobilization, such as adsorption, covalent cross-linking, sol-gel and electropolymerization [11]. Electropolymerization has many advantages: it is a simple process with low cost and anti-interference properties, and it can be widely used in developing enzyme sensors. Pyrrole [12], aniline [13], the organic dye thionine [14] and toluidine blue [15, 16] have been used for the immobilization of enzymes by electropolymerization in the preparation of enzyme sensors.

To date, graphene that is non-covalently functionalized by organic dye electron mediators for use in enzyme sensors has not been reported. In this paper, we describe the development of an electrochemical enzyme sensor that was successfully fabricated by non-covalently functionalizing graphene with TB, and electropolymerizing TB in the presence of horseradish peroxidase (HRP) onto a glassy carbon electrode (GCE) surface. On one hand, the high conductivity of graphene is beneficial for rapid and effective electron transference, which can improve the sensitivity of the enzyme electrode. On the other hand, a large amount of electron mediators and HRP can be loaded onto the large surface of graphene, which can further improve the sensitivity of the enzyme electrode. The analytical performances of this sensor were evaluated for the detection of hydrogen peroxide.

## 2. EXPERIMENTAL

### 2.1 Reagents and instruments

Electrochemical experiments were conducted on a CHI 660C workstation (CH Instruments Co., Shanghai, China) with a modified glass carbon electrode (GCE, diameter 3 mm) as the working electrode, a platinum electrode as an auxiliary electrode, and a Ag/AgCl electrode as a reference electrode. A JSM-6701F field emission scanning electron microscope (JEOL, Japan) was used for scanning electron microscope (SEM) imaging.

Toluidine blue was purchased from Sangon Biotech (Shanghai) Co., Ltd. Graphite powder and hydrogen peroxide were purchased from Xilong Chemical Industry Incorporated Co., Ltd.

(Guangdong, China). Horseradish peroxidase was purchased from Sanjie Biological Technology Co., Ltd. (Shanghai, China).

## 2.2 Preparation of graphene-toluidine blue (Gr-TB) composites

Graphene oxide was prepared by a modified Hummers method [17] with graphite powder as previously described [18]. Hydrazine was added to reduce the graphene oxide to graphene. The Gr-TB composites were obtained by sonicating the mixture of graphene ( $1 \text{ mmol}\cdot\text{L}^{-1}$ ) and toluidine blue ( $0.5 \text{ mmol}\cdot\text{L}^{-1}$ ) for 24 h, followed by extensive washing with distilled water after centrifugation. Finally, Gr-TB was dialyzed against distilled water for 24 h to remove unreacted toluidine blue.

## 2.3 Preparation of modified electrodes

Prior to the modification, GCE was cleaned as described in the reference. The Gr-TB/GCE-modified electrode was obtained by the dropwise addition of  $0.5 \mu\text{l}$  of Gr-TB onto the cleaned GCE surface, then drying it at room temperature and washing it with distilled water.

A solution of  $0.5 \text{ mmol}\cdot\text{L}^{-1}$  toluidine blue and  $3 \text{ mg}\cdot\text{mL}^{-1}$  horseradish peroxidase in phosphate buffer ( $0.2 \text{ mol}\cdot\text{L}^{-1}$ , pH 6.5) was sonicated until the enzyme was completely dissolved. The electrochemical entrapment of HRP into the poly toluidine blue (PTB) network on the Gr-TB/GCE surface was performed in the above solution by electropolymerization using cyclic voltammograms (CV) in a potential range between  $-0.7$  and  $0.8 \text{ V}$  during 20 cycles at a scan rate of  $100 \text{ mV/s}$ . The modified electrode, referred to as PTB-HRP/Gr-TB/GCE, was then washed with distilled water and maintained in PBS ( $0.2 \text{ mol}\cdot\text{L}^{-1}$ , pH 7) at  $4^\circ\text{C}$ . The PTB-HRP/Gr/GCE was prepared with the same procedure as for PTB-HRP/Gr-TB/GCE but with Gr instead of Gr-TB.

## 2.4 Electrochemical measurements

Cyclic voltammograms were obtained using a CHI 660C workstation. A conventional three-electrode system was employed in a range from  $0.4 \sim -0.7 \text{ V}$  in a PBS solution ( $0.2 \text{ mol}\cdot\text{L}^{-1}$ ) to acquire the cyclic voltammograms (scan rate =  $100 \text{ V}\cdot\text{s}^{-1}$ ). The electrochemical impedance spectroscopy (EIS) measurements were performed in  $5.0 \text{ mmol}\cdot\text{L}^{-1} \text{ K}_3[\text{Fe}(\text{CN})_6]/\text{K}_4[\text{Fe}(\text{CN})_6]$  (1:1). EIS measurements were recorded in a frequency range from 1 to 100,000 Hz in the form of complex plane diagrams (Nyquist plots). A constant potential was maintained for the amperometric detection of hydrogen peroxide with the modified electrode as the working electrode.

# 3. RESULTS AND DISCUSSION

## 3.1 Morphological characterization of Gr and Gr-TB

The surface morphology of Gr was examined using SEM to confirm its successful preparation. Figure 1A shows a rough surface with an obvious and typical wrinkled sheet structure. UV-Vis

spectroscopy of Gr was also performed and is shown in Figure 1B. The Gr exhibited an absorption peak at 284 nm, which was the typical UV-Vis spectroscopy of Gr, corresponding to the  $\pi \rightarrow \pi^*$  transition of the aromatic C–C bonds [19]. The UV-Vis spectrum of TB produced two absorption peaks at approximately 288 and 630 nm, which were similar to the peaks obtained in the reference [20]. Two characteristic absorption peaks of TB and Gr were observed in the case of Gr-TB, indicative of the presence of TB on Gr.

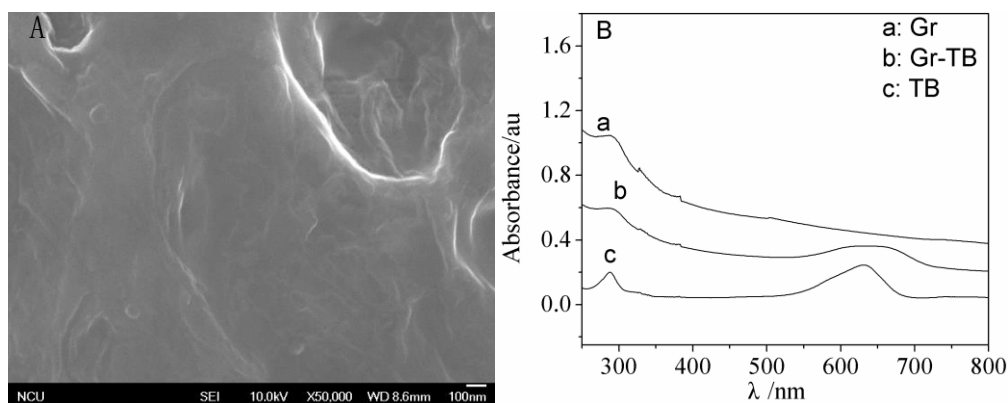


**Figure 1.** (A) SEM image of Gr; (B) UV-Vis spectroscopy of (a) Gr, (b) Gr-TB and (c) TB

### 3.2 Electropolymerization of TB on a GC electrode surface

As shown in Figure 2, 20 consecutive cyclic voltammograms that were recorded by TB electropolymerization on the surface of the Gr-TB/GCE electrode were conducted in a potential range from -0.7 to 0.8 V at a scan rate of 100 mV/s. Figure 2A shows that the anodic and cathodic peak currents increased continuously during cycling, with shape variations that are in agreement with previous literature results [21, 22]. As a result of continuous CV potential cycling, PTB-HRP was deposited on the Gr-TB/GCE surface. The inset in Figure 2A shows the cyclic voltammogram of PTB-HRP/Gr-TB/GCE that was conducted in PBS, pH 7.0. It can be seen that the reduction peak potential was -0.380 V and the oxidation peak potential was -0.237 V.

### 3.3 Electrochemical characterization of the modified electrode

EIS was used to monitor the preparation of PTB-HRP/Gr-TB/GCE using  $[\text{Fe}(\text{CN})_6]^{4-/3-}$  as the redox probe. The Nyquist plots for different electrodes were shown in Figure 2B, which consisted of the linear portion at lower frequencies corresponding to a diffusion limiting process and the semicircle portion at higher frequencies corresponding to the electron transfer limited process. The semicircle diameter equaled the electron transfer resistance ( $R_{ct}$ ), which was varied with different substances modified on the electrode surface [23]. As shown in Figure 2B, the bare GCE produced a small semicircle (curve a). When the electrode surface was modified with a layer of Gr-TB, the diameter of the semicircle decreased slightly (curve b), indicating that Gr-TB facilitated electron transfer between

the  $[\text{Fe}(\text{CN})_6]^{4-/3-}$  and the electrode surface. When PTB-HRP was electropolymerized on the Gr-TB/GCE, the electron transfer impedance was reduced (curve c), indicating that electron transfer from  $[\text{Fe}(\text{CN})_6]^{4-/3-}$  to the surface of GCE can be promoted by PTB [24]. This demonstrates that PTB-HRP was successfully immobilized onto the surface of the Gr-TB/GCE modified electrode.

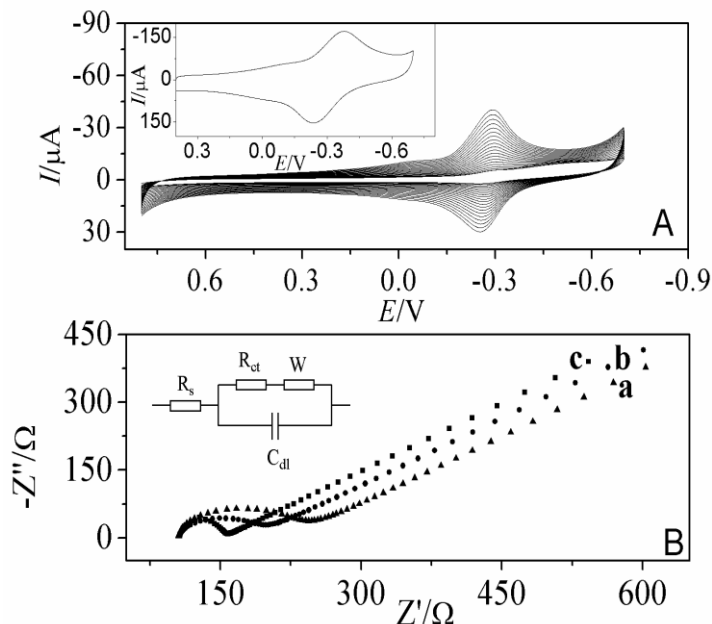


**Figure 2.** (A) Cyclic voltammograms recorded during the electropolymerization of TB. The inset shows the cyclic voltammogram for PTB-HRP/Gr-TB/GCE in PBS (pH 7.0), scan rate:  $100 \text{ mV}\cdot\text{s}^{-1}$ ; (B) EIS response for PTB-HRP/Gr-TB/GCE in  $5.0 \text{ mmol}\cdot\text{L}^{-1} \text{ K}_3[\text{Fe}(\text{CN})_6]/\text{K}_4[\text{Fe}(\text{CN})_6]$  ( $\text{V} : \text{V} = 1 : 1$ ); (a) GCE, (b) Gr-TB/GCE, (c) PTB-HRP/Gr-TB/GCE. The inset shows the equivalent EIS circuit.

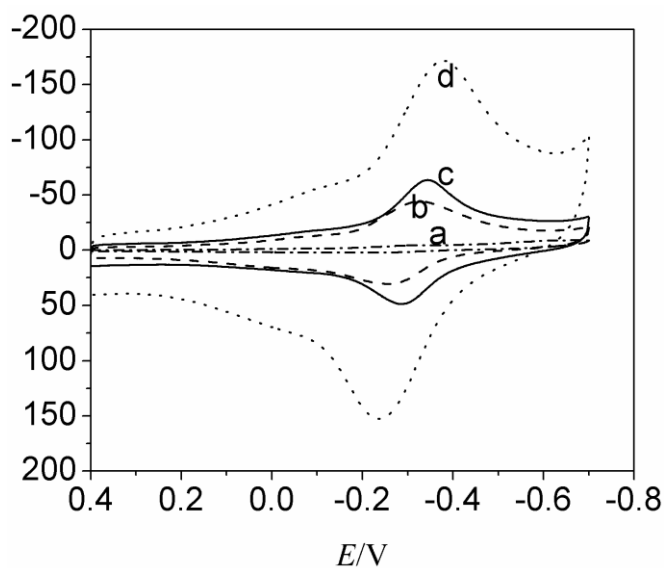


**Figure 3.** Cyclic voltammograms of the different electrodes in  $0.2 \text{ mol}\cdot\text{L}^{-1} \text{ PBS}$ ; scan rate:  $100 \text{ mV}\cdot\text{s}^{-1}$ , (a) PTB-HRP/GCE, (b) PTB-HRP/Gr/GCE, (c) Gr-TB/GCE, (d) PTB-HRP/Gr-TB/GCE.

The CV curves for PTB-HRP/GCE (curve a), PTB-HRP/Gr/GCE (curve b), Gr-TB/GCE (curve c) and PTB-HRP/Gr-TB/GCE (curve d) in  $0.2 \text{ mol}\cdot\text{L}^{-1}$  PBS (pH 7.0) are shown in Figure 3. After the GCE was modified with PTB-HRP by the electropolymerization method, there appeared a pair of weak redox peaks (curve a). When PTB-HRP was immobilized onto the Gr/GCE surface, the charging current of the electrode was increased, and more obvious reversible peaks were observed. Similarly, after PTB-HRP was immobilized onto the Gr-TB composite-modified GCE, the redox peaks increased significantly. Compared with PTB-HRP/Gr/GCE and Gr-TB/GCE, PTB-HRP/Gr-TB/GCE produced the maximum redox peaks. This demonstrates that Gr-TB composites can effectively enlarge the electrode surface areas and facilitate the electropolymerization of PTB-HRP [25].

### 3.4 Effect of pH and potential on the response of the modified electrode

The pH has a great influence on the electrochemical activity of the enzyme and on the response of the biosensor. Therefore, choosing the appropriate pH value could allow the modified electrode to increase its electrocatalytic performance. Consistent with the biological activity of HRP, the amperometric response of the modified electrode was determined in a pH range of 5.5 ~ 8.0 with  $0.50 \text{ }\mu\text{mol}\cdot\text{L}^{-1}$   $\text{H}_2\text{O}_2$ . As shown in Figure 4A, the response current increased at first, and later decreased with increasing pH. At pH 7.0, the modified electrode produced the maximum response to hydrogen peroxide, which was ascribed to the higher activity of HRP in neutral solution [26]. The pH value of 7.0 was in accordance with that obtained for soluble HRP [27]. Therefore, pH 7.0 was chosen as the pH for the test solution.

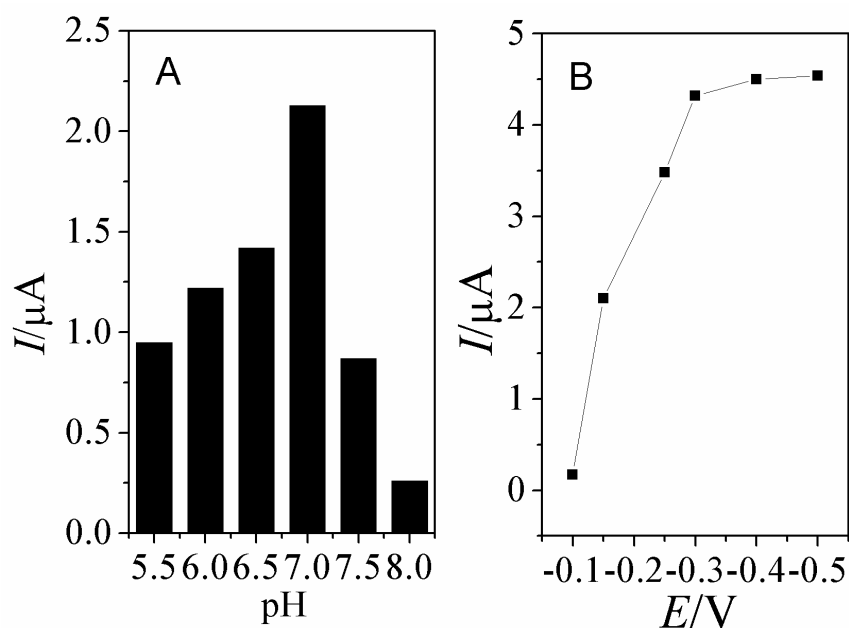


**Figure 4.** (A) Effect of pH on the response of the modified electrode; (B) effect of the work potential on the response of the modified electrode

The influence of the work potential of chronoamperometry on the amperometric response of the modified electrode was evaluated using  $1.0 \mu\text{mol}\cdot\text{L}^{-1}$   $\text{H}_2\text{O}_2$  in solution (pH 7.0). As shown in Figure 4B, from 0.1 to -0.3 V, the current response increased with a negative shift of the applied potential, which was ascribed to the greater driving force for the fast reduction of  $\text{H}_2\text{O}_2$  at a lower potential. When the work potential was more negative than -0.4 V, there was no significant difference in the current response. Therefore, -0.3 V was chosen as the work potential for the amperometric detection of  $\text{H}_2\text{O}_2$ . The potential of -0.3 V was more positive than that of reported HRP biosensors for the detection of  $\text{H}_2\text{O}_2$  [28, 29].

### 3.5 Catalytic performances of the biosensor

To compare the catalytic performances of different electrodes, PTB/GCE, PTB/Gr-TB/GCE, HRP-PTB/Gr/GCE and HRP-PTB/Gr-TB/GCE were prepared and used for the detection of hydrogen peroxide using the chronoamperometric method. The responses of these four electrodes were measured in  $0.2 \text{ mol}\cdot\text{L}^{-1}$  PBS (pH 7.0) with successive additions of  $0.5 \mu\text{mol}\cdot\text{L}^{-1}$  hydrogen peroxide. It can be seen in Figure 5a that the maximum response current among these electrodes was obtained with HRP-PTB/Gr-TB/GCE (d), followed by HRP-PTB/Gr/GCE (c), indicating that the sensitivity-enhancing effect of TB and graphene composites for hydrogen peroxide was significant. The catalytic effect of horseradish peroxidase on hydrogen peroxide can be observed by comparing the response current of PTB/Gr-TB/GCE (b) with that of HRP-PTB/Gr-TB/GCE (d).

The catalytic performance of PTB-HRP/Gr-TB/GCE on hydrogen peroxide was also studied using cyclic voltammetry. As shown in Figure 5B, curve (a) indicates the CVs of PTB-HRP/Gr-TB/GCE in  $0.2 \text{ mol}\cdot\text{L}^{-1}$  PBS (pH 7.0);  $5.0 \mu\text{mol}\cdot\text{L}^{-1}$  hydrogen peroxide was added to the PBS solution to obtain curve (b). Comparing curves (a) and (b), due to the addition of hydrogen peroxide, the cathodic peak current increased and the anodic peak current decreased, indicating that the modified electrode promoted the catalytic reduction of hydrogen peroxide [23].

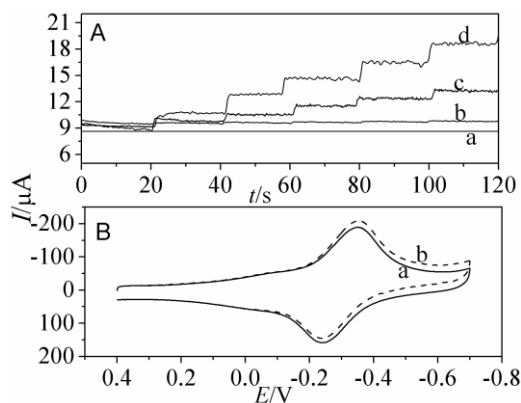


**Figure 5.** (A) Amperometric responses of different electrodes to successive additions of  $0.5 \mu\text{mol}\cdot\text{L}^{-1}$   $\text{H}_2\text{O}_2$  in  $0.2 \text{ mol}\cdot\text{L}^{-1}$  PBS; applied potential -0.3 V, (a) PTB/GCE, (b) PTB/Gr-TB/GCE, (c) PTB-HRP/Gr/GCE, (d) PTB-HRP/Gr-TB/GCE; (B) Cyclic voltammograms of PTB-HRP/Gr-TB/GCE in  $0.2 \text{ mol}\cdot\text{L}^{-1}$  PBS, (a) without  $\text{H}_2\text{O}_2$ ; (b)  $5 \mu\text{mol}\cdot\text{L}^{-1}$   $\text{H}_2\text{O}_2$ , scan rate:  $100 \text{ mV}\cdot\text{s}^{-1}$ .

The cyclic voltammetry curves for PTB-HRP/Gr-TB/GCE in  $0.2 \text{ mol}\cdot\text{L}^{-1}$  PBS (pH 7) at different scan rates ( $10 \sim 600 \text{ mV}\cdot\text{s}^{-1}$ ) are shown in Figure 6. The results show that at scan rates of  $10$  to  $600 \text{ mV}\cdot\text{s}^{-1}$ , the redox peak exhibited a linear relationship with the scan rate. Linear equations for  $I_{\text{PA}}$  (A):  $-2.233\times 10^{-6} - 8.223\times 10^{-3}v$  ( $v\cdot\text{s}^{-1}$ ) ( $R = 0.992$ );  $I_{\text{PC}}$  (a):  $9.746\times 10^{-6} - 7.564\times 10^{-3}v$  ( $v\cdot\text{s}^{-1}$ ) ( $R=0.997$ ), which indicates that electron transfer with the modified electrode was controlled by the surface characteristics.

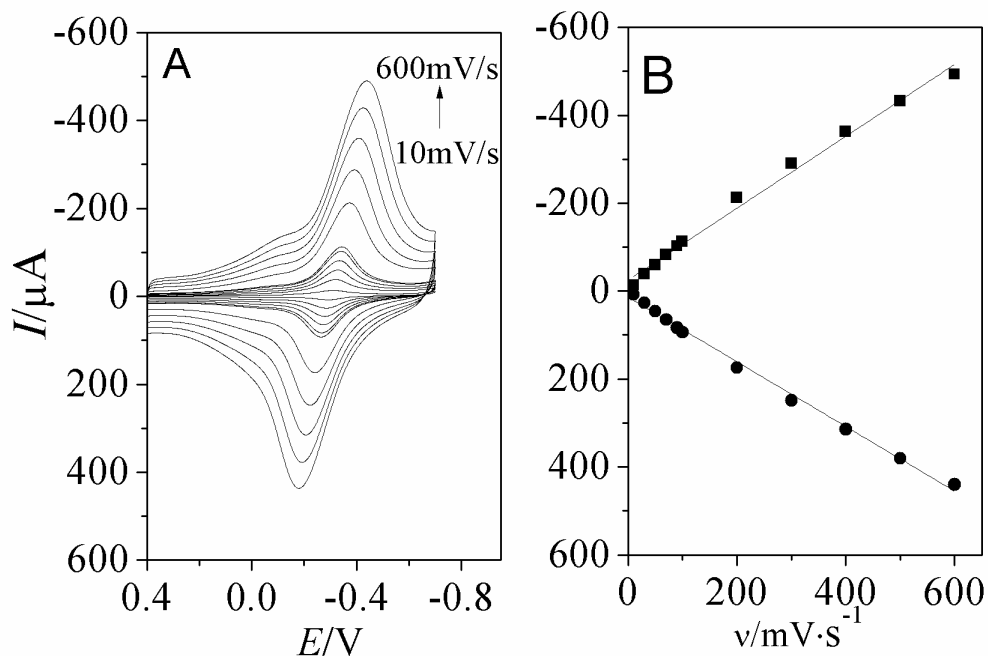


**Figure 6.** (A) CV of HRP-PTB/TB-Gr/GCE in  $0.2 \text{ mol}\cdot\text{L}^{-1}$  PBS at scan rates of  $100 \text{ mV}\cdot\text{s}^{-1}$  to  $600 \text{ mV}\cdot\text{s}^{-1}$ ; (B) the linear relationship between the peak current and the scan rate

The amperometric response of the modified electrode was measured by chronoamperometry in  $0.2 \text{ mol}\cdot\text{L}^{-1}$  PBS (pH 7) under optimal conditions for pH and work potential following successive additions of  $0.50 \text{ }\mu\text{mol}\cdot\text{L}^{-1}$  hydrogen peroxide. As shown in Figure 7A, the addition of hydrogen peroxide produced significant changes in the amperometric response. The modified electrode responded quickly, within 3 seconds, reaching 95% of the steady-state current. The current produced a good linear relationship with the concentration of hydrogen peroxide. As seen in Figure 7B, the modified electrode responded to hydrogen peroxide within a linear range from  $5.0 \times 10^{-7}$  to  $1.35 \times 10^{-5} \text{ mol}\cdot\text{L}^{-1}$ , and generated the calibration curve  $I(\mu\text{A}) = 0.69 + 4.32c$  ( $\mu\text{mol}\cdot\text{L}^{-1}$ ) ( $R=0.999$ ). Based on the batch standard deviation of the blanks, the calculated detection limit of the sensor is  $3.5 \times 10^{-7} \text{ mol}\cdot\text{L}^{-1}$  ( $S/N=3$ ). Table 1 lists the analytical parameters from this work and from those reported in the literature for the determination of hydrogen peroxide with HRP biosensors. It can be seen that the sensitivity obtained in this work was much higher than those reported in the literature, because the Gr-TB composites can effectively enlarge the electrode surface areas and improve the sensitivity of the modified electrode.

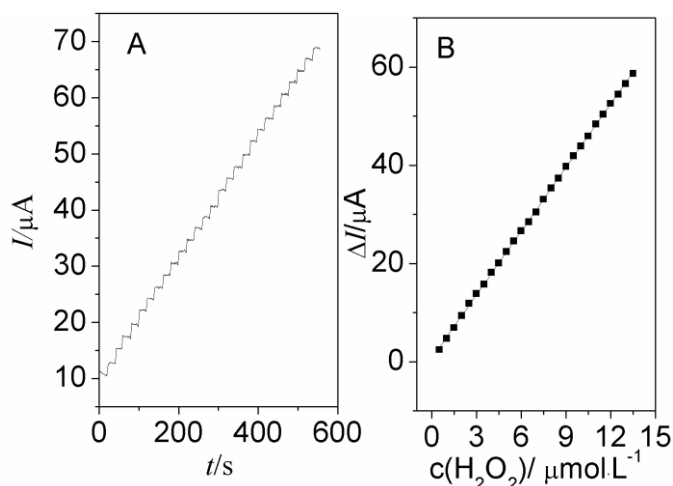


**Figure 7.** (A) The amperometric response of the modified electrode to successive additions of  $0.50 \mu\text{mol}\cdot\text{L}^{-1}$   $\text{H}_2\text{O}_2$ ; applied potential,  $-0.3 \text{ V}$ ; (B) the linear relationship between the current response of the modified electrode and the  $\text{H}_2\text{O}_2$  concentration; applied potential,  $-0.3 \text{ V}$

**Table 1.** Analytical performances of different HRP biosensors for the determination of hydrogen peroxide

Electrode	Linear range ( $\mu\text{mol}\cdot\text{L}^{-1}$ )	Detection limit ( $\mu\text{mol}\cdot\text{L}^{-1}$ )	Sensitivity ( $\mu\text{A}\cdot\text{L}\cdot\mu\text{mol}^{-1}$ )	Reference
HRP/TB/CCB	0.424-360	0.17	0.071	30
HRP/HPC-Fc/GCE	0.1-8	0.1	0.00421	31
HRP/MT-MWCNT/GCE	9-1000	4.0	0.00266	32
HRP/BSA/SPCNTE	5-100	0.85	0.104	33
PTMSPA@GNRs/HRP/ITO	10-1000	0.06	0.021	34
HRP/Au/PDDA/GO/CS/GCE	0.0198-1.04	0.0075	0.55	35
HRP-PTB/TB-Gr/GCE	0.50-13.5	0.35	4.32	This work

CCB: ceramic composite biosensor; HPC-Fc: ferrocene functionalized hydroxypropyl cellulose; MT-MWCNT: maize tassel- multiwalled carbon nanotube; SPCNTE: screen-printed carbon nanotubes electrode; PTMSPA: poly(N-[(3-trimethoxy silyl)propyl] aniline); GNRs: Gold nanorods; GO: graphene oxide; CS: chitosan

### 3.6 Interference, stability and reproducibility

Interference during the use of the modified electrode was evaluated using urea, glycine (Gly), histidine (His) and tyrosine (Try). Interference by PTB-HRP/Gr-TB/GCE was investigated by recording the response during the continuous addition of potentially interfering substances at 10 times the concentration of hydrogen peroxide and hydrogen peroxide ( $0.5 \mu\text{mol}\cdot\text{L}^{-1}$ ) in  $0.2 \text{ mol}\cdot\text{L}^{-1}$  PBS (pH 7.0). As shown in Figure 8, the interference caused by urea, glycine, histidine and tyrosine in the determination of hydrogen peroxide was negligible.

To address practical applications of the modified electrode for the determination of hydrogen peroxide, a recovery test was conducted using samples containing several concentrations of hydrogen peroxide. The concentration of  $\text{H}_2\text{O}_2$  were determined by the standard addition method in  $0.2 \text{ mol}\cdot\text{L}^{-1}$  PBS (pH 7.0). The results listed in Table 2 show recovery values between 97.8 ~ 110.0%.

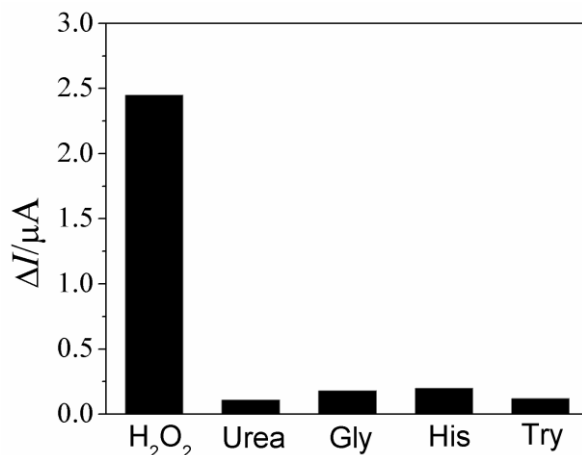


**Figure 8.** Response currents for PTB-HRP/Gr-TB/GCE on successive additions of interferents and H<sub>2</sub>O<sub>2</sub> in 0.2 mol·L<sup>-1</sup> PBS, applied potential: -0.3 V

**Table 2.** Recovery results of the modified electrode for the determination of hydrogen peroxide

C <sub>Original</sub> (μmolL <sup>-1</sup> )	C <sub>Added</sub> (μmolL <sup>-1</sup> )	C <sub>Found</sub> (μmolL <sup>-1</sup> )	Recovery
1.0	A 3.0	3.3	110.0%
3.0	4.5	4.4	97.8%
6.0	6.0	6.1	101.7%

The PTB-HRP/Gr-TB/GCE that was prepared using the same GCE five times was used to determine the amperometric response for 1.0 μmol·L<sup>-1</sup> hydrogen peroxide and the relative standard deviation was 1.3%. The same PTB-HRP/Gr-TB/GCE was used to determine the amperometric response for 1.0 μmol·L<sup>-1</sup> hydrogen peroxide for ten times, and the relative standard deviation was 3.4%, indicating that the electrode exhibits good reproducibility [36]. The modified electrode was maintained at 4°C for four weeks to determine its stability by determining the amperometric response for 1.0 μmol·L<sup>-1</sup> H<sub>2</sub>O<sub>2</sub>. Greater than 80% of the original amperometric response was retained, indicating that the electrode had good stability.

#### 4. CONCLUSIONS

In this paper, we describe the development of a highly sensitive sensor for hydrogen peroxide that was produced by immobilization of HRP through electropolymerization of toluidine blue. This sensor was based on a GCE surface that was non-covalently modified with graphene that was functionalized by the electron mediator toluidine blue. Graphene-toluidine blue composites were characterized by UV-Vis spectroscopy. Preparation of the electrode was monitored by electrochemical impedance. The catalytic performances of the sensor for hydrogen peroxide were evaluated by cyclic voltammetry and chronoamperometry. The results demonstrated that the functionalized graphene can

significantly improve the sensitivity of the HRP electrode. In addition, we explored the effects of pH and the work potential on the electrode's response. The linear range of the HRP electrode for hydrogen peroxide was from  $5.0 \times 10^{-7}$  to  $1.35 \times 10^{-5}$  mol·L<sup>-1</sup> with a sensitivity of 4.32 A·L·mol<sup>-1</sup> and a detection limitation of  $3.5 \times 10^{-7}$  mol·L<sup>-1</sup>.

#### ACKNOWLEDGMENTS

This work was financially supported by the National Natural Science Foundation of China (21465012), the Natural Science Foundation of Jiangxi Province of China (20171BAB203017), and the Scientific Research Fund of Jiangxi Provincial Education Department (GJJ150544).

#### References

1. X.Q. Liu, R. Yan, J. Zhu, J.M. Zhang, X.H. Liu, *Sens. Actuat. B-Chem.*, 209 (2015) 328.
2. V. Sethuraman, P. Muthuraja, J.A. Raj, P. Manisankar, *Biosens. Bioelectron.*, 84 (2016) 112.
3. C. Chen, W. Zha, D. Lu, H. Zhang, W. Zheng, *Mater. Res. Bull.*, 46 (2011) 583.
4. B. Hu, R. Quhe, C. Chen, F. Zhuge, X. Zhu, S. Peng, X. Chen, L. Pan, Y. Wu, W. Zheng, Q. Yan, J. Lu, R. Li, *J. Mater. Chem.*, 22 (2012) 16422.
5. D. Zhang, L. Fu, L. Liao, B. Dai, R. Zou, C. Zhang, *Electrochim. Acta*, 75 (2012) 71.
6. L. Zhu, L. Luo, Z. Wang, *Biosens. Bioelectron.*, 35 (2012) 507.
7. D. Zhang, L. Fu, L. Liao, N. Liu, B. Dai, C. Zhang, *Nano. Res.*, 5 (2012), 875.
8. D. Wang, Y. Li, P. Hasin, Y. Wu, *Nano. Res.*, 4 (2011) 124.
9. X. Dong, L. Yuan, Y. Liu, M. Wu, B. Liu, Y. Sun, Y. Shen, Z. Xu, *Talanta*, 170 (2017) 502.
10. S. Xie, R. Yuan, Y. Chai, L. Bai, Y. Yuan, Y. Wang, *Talanta*, 98 (2012) 7.
11. A.K. Sarma, P. Vatsyayan, P. Goswami, S.D. Minteer, *Biosens. Bioelectron.*, 24 (2009) 2313.
12. I.M. Apetrei, C. Apetrei, *Sens. Actuat. B-Chem.*, 178 (2013) 40.
13. X.Q. Liu, J. Zhu, X.H. Huo, R. Yan, D.K.Y. Wong, *Anal. Chim. Acta*, 911 (2016) 59.
14. S.M. Yang, A.H. Huang, Z.P. Wei, D. Jiang, L.Z. Zheng, *Acta Chim. Sinica*, 18 (2011) 2143.
15. M. Li, L.M. Lu, S.P. Wang, F.L. Qu, X.B. Zhang, S. Huan, G.L. Shen, R.Q. Yu, *Electroanalysis*, 21 (2009) 1152.
16. W. Wang, F. Wang, Y. Yao, S. Hu, K.K. Shiu, *Electrochim. Acta*, 55 (2010) 7055.
17. D.C. Marcano, D.V. Kosynkin, J.M. Berlin, A. Sinitskii, Z. Sun, A. Slesarev, W. Lu, J.M. Tour, *ACS Nano.*, 4 (2010) 4806.
18. R.D. Daniel, M. Shanthi, W.Z. Yan, S.R. Rodney, W.B. Christopher, *Mater. Chem.*, 21 (2011) 3443.
19. M. Jana, S. Saha, P. Khanra, N.C. Murmu, S.K. Srivastava, T. Kuila, J.H. Lee, *Mat. Sci. Eng. B-Adv.*, 186 (2014) 33.
20. J. Liu, A. Zou, B. Mu, *Colloid. Surface B*, 75 (2010) 496.
21. Y.J. Chang, A.P. Periasamy, S.M. Chen, *Int. J. Electrochem. Sci.*, 6 (2011) 4188.
22. D. Gligor, A. Walcarius, *J. Solid State Electrochem.*, 18 (2014) 1519.
23. A.J.S. Ahammad, A.A. Shaikh, N.J. Jessy, T. Akter, A.A. Mamun, P.K. Bakshi, *J. Electrochem. Soc.*, 162 (2015) B52.
24. N. Li, H. Zhao, R. Yuan, K. Peng, Y. Chai, *Electrochim. Acta*, 54 (2008) 235.
25. H. Li, H. Wen, S.C. Barton, *Electroanalysis*, 24 (2012) 398.
26. L. Wang, E. Wang, *Electrochem. Commun.*, 6 (2004) 225.
27. S.Q. Liu, H.X. Ju, *Anal. Biochem.*, 307 (2002) 110.
28. S.Z. Bas, H. Gulce, S. Yildiz, A. Gulce, *Talanta*, 87 (2011) 189.
29. H. Zhang, X. Hu, X. Fu, *Biosens. Bioelectron.*, 57 (2014) 22.
30. K. Thenmozhi, S.S. Narayanan, *Mat. Sci. Eng. C-Mater.*, 70 (2017) 223.

31. P. Li, H. Kanga, C. Zhang, W. Li, Y. Huang, R. Liu, *Carbohydr. Polym.*, 140 (2016) 35.
32. M. Moyo, J.O. Okonkwo, N.M. Agyei, *Electroanalysis*, 25 (2013) 1946.
33. S. Xu, X. Qin, X. Zhang, C. Zhang, *Microchim. Acta*, 182 (2015) 1241.
34. S. Komathi, A.I. Gopalan, S.K. Kim, G.S. Anand, *Electrochim. Acta*, 92 (2013) 71.
35. C. Yu, L. Wang, W. Li, C. Zhu, N. Bao, H. Gu, *Sens. Actuat. B-Chem.*, 211 (2015) 17.
36. X.B. Kang, G.C. Pang, X.Y. Liang, M. Wang, J. Liu, W.M. Zhu, *Electrochim. Acta*, 62 (2012) 327.

© 2017 The Authors. Published by ESG ([www.electrochemsci.org](http://www.electrochemsci.org)). This article is an open access article distributed under the terms and conditions of the Creative Commons Attribution license (<http://creativecommons.org/licenses/by/4.0/>).